THESIS FOR THE DEGREE OF LICENTIATE OF ENGINEERING

Net-Shape Consolidation of Water-Atomised and Gas-Atomised Steel Powder Towards Full Density

ANOK BABU NAGARAM

CHALMERS

Department of Industrial and Materials Science

CHALMERS UNIVERSITY OF TECHNOLOGY

Gothenburg, Sweden, 2022

Net-Shape Consolidation of Water-Atomised and Gas-Atomised Steel Powder Towards Full Density

ANOK BABU NAGARAM

Technical report no IMS-2022-2

Licentiate Thesis at Chalmers University of Technology

Department of Industrial and Materials Science

Chalmers University of Technology

SE-412 96 Gothenburg

Sweden

Tel: +46 (0)31 772 1244

Printed by Chalmers Reproservice

Gothenburg, Sweden 2022

Net-Shape Consolidation of Water-Atomised and Gas-Atomised Steel Powder Towards Full Density

Anok Babu Nagaram
Department of Industrial and Materials Science
Chalmers University of Technology

Abstract

Powder metallurgy (PM) provides resource- and cost-efficient routes to create near-net shape products compared to conventional metal fabrication techniques. To improve the mechanical performance of PM steels, it is a prerequisite to enhance the density of the material. Utilizing cold isostatic pressing (CIP) process allows to isostatically compact and eliminate the otherwise needed organic lubricants used for the powder compaction resulting in homogeneous distribution of density. To reach full density, HIP is an attractive final stage and so in particular if the HIP can be done capsule-free directly on a sintered component. Hence, combining CIP, sintering and capsule-free HIP means that full density processing of novel products can be achieved. Chromium-alloyed PM steels have been developed with the benefit of lower cost owing to the lesser use of alloying elements such as Ni, Cu and Mo. PM steel powder grades contain Fe-rich oxide mostly covering the surface of powder particles. It is of outermost importance to sinter the material prior to final capsule-free HIP to largely remove the surface oxides to eliminate possible transfer of oxygen to trigger added formation of Cr-oxide during the sintering. The test materials used in this thesis study are water-atomised steel powder grades prealloyed with 1.8%Cr and admixed 0.3% graphite and with 2%Ni and gas-atomised Vanadis 4E tool steel powder grade. While Cr-alloyed PM steel powder grade is isostatically pressed directly from virgin powder to densify the green compacts, granules of Vanadis 4E were needed for the this and produced before CIP. Results show that after sintering at high temperatures either in reducing or vacuum conditions for water-atomised steel powder grade, most of the surface pores are eliminated and nominally full bulk density is achieved after capsule-free HIP. A novel approach is also explored investigated to sinter the Cr-alloyed PM steel in HIP furnace and followed by capsule-free to approach high densification. Microstructures of these compacts sintered at 1250 °C revealed the complete closure of surface pores, after which densification to nominally full bulk density has been achieved by the final capsule-free HIP stage. Following the route of CIP, sintering and capsule-free HIP, nominally full density is also achieved for the Vanadis 4E tool steel when CIP compacting the powder in granulated condition.

Keywords:

Powder metallurgy, PM steel, Prealloyed with Cr PM steel, high temperature sintering, sintering atmosphere, high density, cold isostatic pressing, hot isostatic pressing

PREFACE

This licentiate thesis is based on the work performed in the Department of Industrial and Materials Science at Chalmers University of Technology from September 2019 to April 2022. The work has been carried out under the supervision of Professor Lars Nyborg and Professor Eduard Hryha. This work has been performed within the framework of project funding from strategic innovation program Metalliska Material through the project DENSE, financed by the Swedish Governmental Agency for Innovation Systems (VINNOVA).

This licentiate thesis comprises an introductory part on powder metallurgy of steels with a review on aspects related to high density approaches using new processing routes.

List of appended papers

I. **Consolidation of Water Atomized Chromium-Nickel-alloyed PM Steel Through Novel Processing Routes**
Anok Babu Nagaram, Maheswaran Vattur Sundaram, Johannes Gårdstam, Michael Andersson, Zhuoer Chen, Eduard Hryha, Lars Nyborg
In Manuscript

II. **Role of nickel addition on sintering and microstructure control of chromium-alloyed steel powder**
Anok Babu Nagaram, Yu Cao, Maheswaran Vattur Sundaram, Michael Andersson, Hans Magnusson, Eduard Hryha, Lars Nyborg
In Manuscript

III. **Effect of process control on the densification of Cr-prealloyed PM steels through vacuum sintering in conjunction with capsule-free hot isostatic pressing**
Anok Babu Nagaram, Johannes Gårdstam, Maheswaran Vattur Sundaram, Michael Andersson, Zhuoer Chen, Eduard Hryha, Lars Nyborg
In Manuscript

Contribution to the appended papers

I. The author planned the work together with co-authors and performed the experimental work, took part in the analysis of the results in collaboration with the co-authors and as well wrote the paper in close cooperation with the co-authors.

II. The author planned and performed the experimental work with co-operation of the co-authors and wrote the in cooperation with the co-authors.

III. The author took part in the planning along with co-authors and performed the characterization and analysis of the results in collaboration with the co-authors.

Table of Contents

CHAPTER 1

INTRODUCTION

1.1. Background

Powder Metallurgy (PM) processing is a net or near-net shape technology developed generally to produce structural and functional metallic parts. The PM technology has grown rapidly due to its uniqueness in delivering products with desired properties in high volume. One of its main characteristics is to make it possible to fabricate complex product shapes in cost effective way. Commonly, the first stage of the PM processing route is compaction/shaping, in which metal particles of micrometre size are joined together by means of applied, often uniaxial pressure. This results in good so-called green strength involving the packing, interlocking and plastic deformation of the metal particles to desired shape and integrity. For this process to work, the metal powder must be irregular in shape, e.g., powder fabricated by means of water atomisation. After desired shape of the compact is realised, follows the heat treatment process known as sintering, usually preceded by debinding. Sintering is performed between 0.5 and 0.7 of melting temperature in Kelvin degrees for the material in question. The sintering is done in controlled reducing atmosphere and during the sintering, sinter necks developing between the metal particles lead to the necessary strength increase. Depending on material, with higher temperatures, the sintering can lead to the closure of pores, i.e., near-full density.

Although metallic parts produced through PM exhibit good dimensional tolerance, their mechanical properties are not comparable to those of wrought steels [1]. One of major constraint is the presence of pores, which deteriorates the strength of the components. At the same time, the need for the requirement of high density of PM parts for automotive applications has grown rapidly over the last years. Various alternative PM methods are in stock to produce high density components. Copper infiltration and powder forging are used for enhancing the final density, but their application is partly hindered by their effects on the physical nature of the component and related added cost of processing and hence final component cost [2].

Reaching high to full density is not possible and feasible through increase of compaction pressure during uniaxial compaction alone. Still, with proper control of alloying elements and sufficient and uniform mixture of lubricant involving e.g., warm compaction or high velocity compaction, followed by high temperature sintering, the former approach can bring the final part to near closed porosity, while

the latter can even result in nominally full densification, but with the sacrifice of shaping capabilities. Proper lubricant must be chosen with respect to their theoretical densities to avoid its effect on the green density of the compacted parts at high compaction pressure. Therefore, in order to avoid the utilization of lubricant, novel processing route has to be investigated. In case of conventional press and sinter route, not only will the die tools and lubricants used affect the cost, but also fabricating complex shapes would be difficult. Hence, cold isostatic pressing (CIP) is a process where these above-mentioned factors are not necessary and constitute an important part of the present licentiate study.

Sinter density of the component is also influenced by powder characteristics such as powder shape and size. Water atomized powder allows to reach high green strength unlike gas atomized powder. This is an effect of the fact that spherical gas-atomised powder simply does not have the interlocking capability as irregular water-atomised powder, when being subjected to high pressure. To enhance the green density during compaction of spherical particles characteristic for gas-atomised powder, methods of granules production such as starch consolidation (SC) and freeze granulation (FG) can be applied. Densification to closed porosity is then attainable after sintering such green components through extensive volumetric shrinkage in sintering atmospheres providing necessary processing conditions. Full densification is thereafter approachable by undergoing the post processing heat treatment such as capsule-free hot isostatic pressing (HIP). These lines of research have also constituted part of the present licentiate thesis. Furthermore, as a consequence of such novel processing route, this is the way forward to reduce processing stages or avoid high cost for tooling without compromising on the mechanical properties. Finally, sintering of the PM components after CIP is potentially also viable in HIP furnace and followed by capsule-free HIP, which constitutes a novel promising approach that also has been explore in the present thesis study. Consequently, there are novel ways to achieve full density for high performance and tool steel applications that widen the investigation to enhance the final properties of PM components.

1.2.Research Objectives

This thesis aims to provide basic understanding of possible processing routes to attain near-full to full density of PM steel to reach improved mechanical and functional properties. The overall approach has been to address methods and approaches along the whole value chain involving the application of high-pressure compaction, lubricant-free cold isostatic pressing (CIP), role of sintering conditions to reach minimum closed porosity prior to final capsule-free hot isostatic pressing to reach pore-free final component. Both water atomized and gas atomized powder grades are

studied using various consolidation and pre-consolidation methods. Specific research questions are as follows:

1. What is effect of compaction pressure, sintering temperature and sintering atmosphere on the densification of Cr-Ni-alloyed PM steel?
2. What is the effect of admixed nickel on the microstructure for Cr-prealloyed PM steel at varying sintering temperatures?
3. What is the effect on densification by sintering in HIP furnace prior to final capsule-free HIP?

CHAPTER 2

POWDER METALLURGY

2.1 Past to current trends in PM technology

Powder metallurgy (PM) has been in use since 3000 B.C. which show-cased its use in prehistoric attractions such as iron pillar in Delhi, monuments during Egyptian era, etc [1]. During this period, it was unknown how the powder was fabricated, but this reduced sponge metal powder was hammered or forged together to make PM tools. Due to absence of knowledge in furnaces then, melting of metals was practically not possible. Metals with low melting points such as gold and bronze were utilized most of times to be used as decorative art. As the years passed, furnaces have advanced in their technology and development of metals having high melting points became possible. In mid-20th century, PM industry has grown rapidly in making automotive parts such as self-lubricant bearing [3]. In current days, PM industry has been widely used in various applications such as automotive [4], fuel cells [5], soft magnetic composites [6], and high performance parts [7].

For decades, PM technology has been recognised in various aspects of being resource efficient. The process of PM is also named as a well-recognised "green" technology in the manufacturing industry and it has been designated as a sustainable manufacturing solution [8], [9]. PM is termed as "green" due to the typical use of recycled scrap metals to produce powder for PM, the near full utilisation of powder to final product and less energy need to produce final parts compared other conventional processes such as casting and forging. Nearly 60% to 70% of the parts produced using PM technology in the world are in automotive industry [10].

For a PM part to be produced with desired properties certain steps must be followed as outlined above, namely compaction, sintering and secondary heat treatment operations. Compaction is the method in which the metal particles are consolidated into a green body of a desired shape. More complex shapes can be fabricated using PM unlike through casting or forging. Sintering is the heat treatment process used for establishing the necking between the metal particles and enhancing the densification behaviour of the alloy processed. Depending on the application, porous to high/full density materials are fabricated. It is possible to tailor the properties from the beginning to the end of the PM processing chain, i.e., from powder fabrication to the post-sintering processing. This particular advantage stands out to be an attractive means to tune the microstructure of the material in each stage of the PM processing

route and can constitute a keyway forward to reach high final relative density, being main prerequisite for high performance parts.

2.2 Fabrication of Metal Powder

Almost all pure and prealloyed grades of metal powder (aluminium, low-alloy steel, tool steel, titanium alloy, nickel alloy and stainless steel) are produced mainly by the process of atomization. Various process types of atomization are available to produce powder such as water atomization, gas atomization, centrifugal atomization, vacuum atomization and ultrasonic atomization [11].

Mostly, low alloy steels are produced using water atomization and high alloy steels as e.g., tool and stainless steels are produced using gas atomization due to their strong affinity towards oxidation. Atomization is the process of breaking up the melt into fine droplets either using water jets or high-pressure gas and solidifying these to form metal particles. Water-atomized powder provides good interlocking between the metal particles contributing to high green strength. Low alloy steel powder exhibits good compressibility whereas high alloy steel powder is difficult to compress and bring to good shape. The morphology of the powder varies from irregular to spherical for water atomization and gas atomization.

Production costs using water atomization is less compared to other atomization methods, but there are constraints due to powder purity with high oxygen content of up to 1 wt.% [12]. Particle shape and size rely on principle parameters such as water pressure in water atomization and nozzle design together with gas pressure in gas atomization. Other parameters that influence the powder characteristics are, atmosphere of atomizer, melting temperature, viscosity, surface tension, superheat of material, etc.

2.3 Alloying methods

During the recent years a lot of effort has been put in developing low alloy PM steel components. Alloying of the materials is done to boost the mechanical properties of the final product. High strength is the main prerequisite property for these steels to be produced to compete with the traditional alloys. Depending upon the nature of alloying elements in the alloy, various procedures have been established to produce low alloy systems and these are as follows.

Admixed Powder Grades

Alloys are produced by mixing elemental powder to the base powder, which does not compromise the compressibility in uniaxially pressing [13]. This is a result of the fact thar the mixture is not a product of prealloyed system, which otherwise increases the resistance to plastic deformation owing to e.g., solution hardening of the metal matrix thus reducing the compressibility. Constituents with weak affinity towards oxygen can with ease be admixed such as graphite, nickel, copper, etc. Nevertheless, degree of alloy homogenisation during sintering is limited due to too slow diffusion of substitutional alloying elements like nickel, etc., at sintering temperature.

Diffusion-alloyed Powder

Fine elemental powder of e.g., nickel, copper and in some cases also molybdenum is admixed to the iron/steel base powder and bonded to the base powder by solid state diffusion process termed diffusion alloying. The bonding is controlled during the diffusion alloying heat treatment with resulting powder mixture known as "partially prealloyed mixture" [14]. This approach is performed to retain the compressibility by restricting the number of elements present in pre-alloyed state of base powder.

Pre-alloyed Powder

Additions of elements to the molten metal in the atomization process results in a chemically uniform distribution of alloying elements in the alloy [15]. Low alloy steel powder with not more than 2 elements is often the case and the composition is specifically formulated for high performance PM parts. Elements that have high affinity towards oxygen such as Cr and Mn are commonly pre-alloyed with base system, iron. The pre-alloying lowers the activity of the elements and compared to having elements like Cr and Mn in elemental powder form constitutes hence less challenge in sintering control.

Hybrid-alloyed Powder

Addition of elemental powder or master alloy powder to either diffusion-alloyed or pre-alloyed powder are called hybrid-alloyed powder systems [16]. These new hybrid-alloy powder grades are formulated to obtain required chemical composition and attain improved microstructure and properties on sintering at high temperatures.

Granulated Powder

Alloy powder that is not possible to compact to necessary green strength due to either alloy system characteristics or their spherical shape, i.e., powder produced by means

of gas atomization, are granulated by mixing with binder resulting in strong green strength after pressing. These granules are free-flowing and do not agglomerate, which can be produced using the technique called freeze granulation [17]. A suspension is sprayed into liquid nitrogen (-196 °C) bath to be freeze-dried. This produces droplets without voids. These droplets are dried in vacuum through sublimation, which helps in the formation of spherical granules. Parameters responsible for the granule size distribution are air pressure, rheology of the suspension and the pump speed used during the spraying stage.

2.4 Powder Compaction

An important aim of PM is to achieve as high relative density of the component as possible. High relative density is a requirement because with increase in density, mechanical properties such as strength, ductility and toughness are significantly improved [18].

Strength of PM steels is improved in number of ways such as:

- Increase in density;
- Strengthening by alloying;
- Strengthening by heat treating the alloyed material.

Alloying the materials with several elements or heat treating the material after sintering may become an expensive process not always allowing to reach required outcome. Thus, methods to increase the density has been investigated widely since few decades.

Compaction of the powder is influenced by the following powder characteristics:

- Particle size;
- Apparent density;
- Flow/fill characteristics;
- Particle hardness;
- Compressibility;
- Green strength.

2.4.1 Uniaxial Compaction

Uniaxial compaction is a widely used method in PM industry for producing structural components. In addition to the above-mentioned parameters in section 2.4, the lubricant admixed with water-atomized powder when filled in the die and compacting uniaxially influences the densification of the powdered material. The use of low density lubricants will take up much of the compact volume, affecting the

reachable sintered density after the removal of lubricant [19]. In conventional pressing process, there is also density gradient caused due to non-uniform pressure distribution within the compact along the die walls, with decreasing gradient along the compaction direction in lateral direction from the surface to the core of the part. This is a result of mainly the friction between the powder and die wall in combination with the effect of interlocking particles, thus having impact on dimensional tolerances after sintering. Although addition of lubricant improves compressibility, reaching high relative density after sintering after uniaxial compaction is not easy [19]–[21]. It is possible to approach uniform distribution of density within the compact by moving the punches relative to another with regards to the desired density of the component having different sections using platens [22].

2.4.2 Delubrication/Debinding

As discussed in earlier section, additive such as lubricants or binders are admixed to the powder to increase the compressibility during the compaction. Depending on the type of additives admixed to the powder in case of Cr-alloyed grades, lubricants or binder are evaporated or decomposed to heavy hydrocarbons at around 350 °C to 450 °C in dry nitrogen atmosphere [23]–[27].

2.4.3 Cold Isostatic Pressing

Cold Isostatic Pressing (CIP) is a process, in which isostatic pressure is applied on the powder body resulting in uniform density distribution within the compact fabricated, normally resulting in low distortions during sintering. The CIP process is carried out using a pressure medium such as liquid or air at between 100 MPa to 600 MPa at room temperature for some minutes, typically e.g., 2 minutes. The CIP process can be performed in two ways (a) wet bag isostatic pressing (b) dry bag isostatic pressing. In the wet bag isostatic pressing process, flexible rubber mould design shaped to final product is filled with powder and the mould is then vacuum sealed in a bag. This bag is placed in the CIP chamber containing pressure medium. In dry bag isostatic pressing process, powder is directly filled into the tool which is fixed to the CIP chamber containing pressure medium. CIP provides an advantage compared conventional pressing as there is no friction between the metal particles and die walls. Hence, there no use of lubricants and process eliminates the residual stresses, provides for economical tooling cost (wet bag), large parts in size (wet bag), compacts with complex shape and in fact comparably high production rate (dry bag). In addition to other PM technologies, CIP process is characterised by low energy consumption, thus low production costs of at least 60% when compared to conventional manufacturing routes recorded [28]–[31].

2.5 Sintering

Sintering is defined as a process of heat treatment aiming at bonding metal particles of a pre-shaped compact at an elevated temperature that is below the melting temperature in the range of 70% to 90% of the melting temperature of the main element in Kelvin degrees. The fundamental driving force of the sintering process is to decrease the surface free energy which is caused by mass transport mechanisms. Sinter necks are formed in the first stage at the contact of metal particles during sintering and grows as the sintering temperature increases with resulting densification due to the predominant mechanism of volume diffusion as well as grain boundary diffusion. In addition, growth of sinter necks depends also on surface diffusion and evaporation/condensation mechanisms, which contribute to transfer of matter to the sinter necks without leading to densification. Surface diffusion and grain boundary diffusion are more rapid diffusion mechanisms that are active at comparably lower temperatures compared to volume diffusion and hence particularly involved in initial sintering stages. In the later stage of sintering, with increase in temperature, pores are not only reduced in number, but also change their morphology to become more rounded [32]. With the increase in sintering temperature, porosity is decreased, i.e. sintered density is improved, thus resulting in enhanced mechanical properties [33].

Grain growth takes place as the pores evolve with increase in sintering temperature. This coarsening of grain size will influence the properties of the material. Thus, controlled microstructure having finer grain size with high density results in the improvement of the sintered properties. Shrinkage of pre-shaped compacts is one of the key factors of sintering, which influences shape and dimensions of the sintered compact. Higher the green density after compaction will lead to lower shrinkage to reach given sintered density and this improves the ability to reach desired final dimensions.

To achieve proper necking between the metal particles during sintering, these must be fully or partially free from surface oxide, otherwise sintered neck formation will be hampered [71]. The role of surface oxide characteristics on sintering of Cr-alloyed steel powder has been extensively studied [68-70]. In conclusion, it is shown that such powder is mainly covered by 3-5 nm Fe-based oxide layer and to minor amount by particulates formed by more stable oxides rich in strong oxide formers as Mn and Cr. Oxide reduction during controlled sintering process helps in achieving effective necking and avoids the growth of thermodynamically stable oxides [34]. Since atmosphere in the furnace greatly affects the compacts during sintering, it must be performed either in inert, reducing, or vacuum conditions. The predominance of Fe-

oxide with respect to surface coverage means that most of the surface oxide can be reduced in an early stage already during the heating state of the sintering, while the Cr- and Mn-rich oxides can only be affected at higher temperatures during the sintering [24], [25], [34], [35].

2.5.1 Gaseous Sintering

The fundamental purpose of controlled atmosphere during sintering is to prevent oxidation and to reduce surface oxides, which results in good bonding between the adjacent metal particles. In Ferrous PM industry, three main sintering atmospheres are traditionally used: reducing-decarbonizing (e.g., cracked ammonia, hydrogen), reducing-carbonizing (e.g., endogas) and neutral (e.g., nitrogen). In modern sintering, nitrogen-hydrogen mixtures are also used. For the reduction of wüstite (FeO) at normal sintering temperature of 1120 °C, the dissociation pressure of about 10^{-12} atm. is required to decompose FeO without active reducing agent, unless done at ultra-high vacuum conditions [24], [36]. Still, as soon as there is hydrogen in the sintering atmosphere the Fe_2O_3 layer on the powder surface is readily reducible at below 400 °C [35]. In case of Cr-prealloyed PM steels, the sintering in hydrogen-containing atmospheres means that action of hydrogen is often not strong enough to impact on the Cr-Mn-oxide particulates, which means that carbothermic reduction driven by the carbon added to provide the carbon level of the material instead becomes decisive [24], [35], [37].

2.5.2 Vacuum Sintering

Absence of gaseous atmosphere during sintering is termed as a process of vacuum sintering. Recent studies showed that Cr-prealloyed PM steels can be well sintered in low vacuum and significant impact on the reduction of oxides have been obtained due to carbothermal reactions occurring at temperatures of above 1000 °C [34], [38]. Materials like titanium, tool steels, stainless steels, and magnetic alloys are sintered in vacuum as these materials react during sintering in atmospheres containing e.g., nitrogen. In case of vacuum sintering, it is important to maintain back pressures at above the vapour pressures of the constituents of the alloy. If not so, sublimation is expected, which influences the material stoichiometry and leads to furnace contamination with changes observed in sintering behaviour [39].

2.6 High Sintering Temperature and Mechanical Properties

Density is one of the main characteristics that influences the materials properties. High performance parts requires enhanced strength which is achieved with high sintered density [1]. There are various approaches to reach high sintered density of materials as discussed in Section 2.4. Previous studies have shown that increase in sintering

temperature for Cr prealloyed PM steels results in higher density [7], [40]; when sintering at 1250 °C densification increases up to 1% of the theoretical density in relation to that at 1120 °C. At the higher temperature, the pores tend to become isolated and show more roundness. The temperature of 1120 °C is otherwise most widely used in industry for sintering PM steels using conveyor belt furnace. Such furnace types are restricted to work at around this lower temperature. Thus, batch furnaces are developed for high sintering temperatures including e.g., low pressure sintering furnaces (low vacuum sintering). It should be noted that with increase in temperature, increased dimensional changes are observed for the same material when sintered either in reducing atmosphere or in vacuum. In addition, increase in temperature also tentatively influence the density of the material as the reduction of stable oxides is eased at higher temperatures for given sintering atmosphere, resulting in stronger neck growth and tentatively improved mechanical properties [19], [41], [42].

2.7 Effect of Ni in Cr-alloyed PM Steels

Although there exist some applications of plain water-atomized iron powder, it is the utmost requirement to alloy the material that enables an enhancement in the mechanical properties of final part. Alloying is a necessary measure to ensure necessary thermal processability and hardenability. As described in Section 2.3, alloying can be done in few ways. Since few decades, Cr-alloyed PM steels have been developed for high performance applications. The Cr is pre-alloyed to the base powder in the atomisation process and the Cr improves the hardenability of the sintered material and hence the achievable strength [43], [44]. Alloying elements such as Ni and Cu are admixed to the Cr-alloyed PM steel by diffusion bonding. Owing to their low affinity to oxygen this constitutes no risk for oxide control. Furthermore, since both elements have solution hardening effect, this approach prevents from reducing the compressibility of the material and while it promotes the hardenability. Hence, Cr-alloyed PM steels having also Ni has inhomogeneous distribution of microstructure with nickel-rich regions besides the main steel microstructure. The Ni rich regions could be detrimental to the mechanical properties [45]. Previous studies have reported the reduction in inhomogeneity distribution of Ni in presence of Cr, with martensite and bainite being promoted which improves the mechanical strength [46], [47].

2.8 Effect of Density and Microstructure on Properties

Many studies have shown that density and microstructure of the PM steels jointly influence the mechanical performance of PM steels [7], [48], [49], [50] . A schematic

representation of the influence of density on different mechanical properties is illustrated in Figure 1 below. The figure clearly shows that at lower density levels typical for conventional press and sinter (range a), the sintered materials exhibit lower properties, in particular toughness related as impact strength and ductility related as elongation to fracture. As density is increased above 7.0 g/cm^3 (range b) and in particular at above 7.5 g/cm^3 all properties are significantly improved.

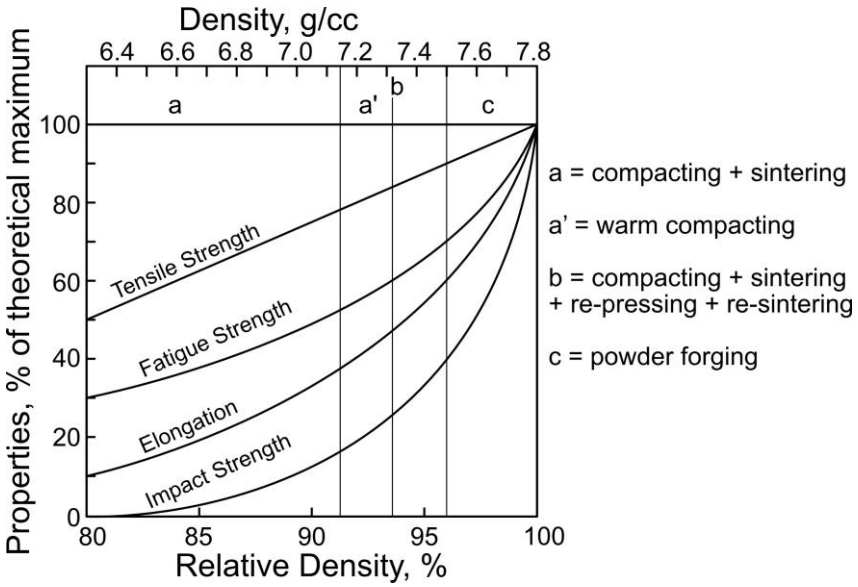

Figure 1. Effect of relative density on the mechanical performance of PM component (redrawn from [50])

With the PM processing route, by tuning from the powder characteristics to the final component through choice of compaction and sintering strategies, tailored microstructure combined with increased sintered density are achievable, resulting in improved mechanical performance. At the end, the microstructure obtained in PM steel relies on composition of the alloy material and the cooling rate applied during sintering as well as the design of post-sintering heat treatment. Applying forced controlled cooling rate in the sintering run is termed sinter hardening and has been demonstrated in particular for PM Steel with 3 wt.% Cr [51]. For grades with lower Cr-content of say 1.8 wt.%, these are most suited for post-sintering heat treatment and possibly case carburising [13]. In essence, depending on the alloying route of powder grade mixtures, microstructures can vary further, for example for Ni-containing diffusion-alloyed PM steel, the heterogeneous microstructure is preserved as the interdiffusion of Ni and Fe is too limited at sintering to provide for complete homogenisation. As a result, Ni-containing PM steel reveals different microconstituents such as martensite, bainite, pearlite, Ni-rich martensite and Ni-rich austenite in a material that exhibits combination of high strength, good toughness without compromising on the toughness [51]–[53].

2.9 Hot Isostatic Pressing

Hot isostatic pressing (HIP) is a process involving the application of high temperature and high isostatic pressure. The pressure is accomplished using inert gas as a transfer medium, also previously referred as "gas pressure bonding". In this process, powder is filled in metallic canister, which is placed in the HIP chamber to obtain full densification by the combined action of temperature and pressure. One of main advantage of the HIP process is achieving fully densified components at lower temperatures (e.g., 1100 °C-1150° C) due to high isostatic pressure when compared to conventional sintering process, for which high temperature sintering (1250 °C or higher) is required to at least reach closed porosity. The HIP procedure helps in preventing or limiting the addition of sintering aids and grain-growth inhibitors. Uniformly dense components are produced with large length-to cross section ratios weighing up to 2 tons reaching full relative density of the material with respect to its theoretical density. In addition, material used for canister should be like the alloy matrix and there is quite some effort to create the canister, making it an expensive process.

2.9.1 Capsule-free Hot Isostatic Pressing

The HIP can be used on the pre-shaped component without using canister. This, however, requires materials prior to HIP that free from surface pores and do not provide pore channels into the part, otherwise achieving full density is not possible. Furthermore, to reach high quality material using capsule-free HIP, it is important to eliminate the effect of oxide content resulting from the surface oxide of the atomized powder. This is in particular important for water-atomized grades that have high surface oxygen content owing to their high specific surface area. Typically, Cr-alloyed steel powder has an oxygen level of 0.15 wt.% [41]. If this oxygen level is not strongly reduced, the result may be deteriorated mechanical properties. This happens when oxide inclusions are present at the contact between the particles, deteriorating the properties such as ductility, fatigue resistance and impact toughness [54]–[57]. Consequently, controlled processing route is required and this can be achieved with precise control along the whole processing route, eliminating surface pores and oxides during the sintering process [58]. This methodology is already applied to parts produced by MIM and sinter-based AM [59]. Although the HIP is done in argon gas for a capsule containing material, it is necessarily not recommended for capsule-free HIP proceeding of a conventionally sintered component. This is because argon might get trapped in the material with risk for residual argon-induced porosity. Hence, new approaches of sintering in vacuum and continuous capsule-free HIP are developed in this thesis.

CHAPTER 3

MATERIALS AND METHODS

This chapter provides a brief overview of the materials, processes and experimental techniques used in this thesis study and their respective background.

3.1 Materials and Processes

3.1.1 CIP Mould Fabrication

In order to create flexible mould for CIP, a novel approach involving the 3D-printing of moulds was developed applying the material extrusion technique fused deposition modelling (FDM). The flexible moulds were in this way fabricated using Thermoplastic Polyurethane (TPU) filament on ZYXX+ FDM printer. The TPU as mould material was chosen to provide appropriate shore hardness for the CIP processing. Trails were made with different printed mould shapes in combination with different thicknesses. As can be seen below in Figure 2 conical, rectangular and screw shapes were fabricated.

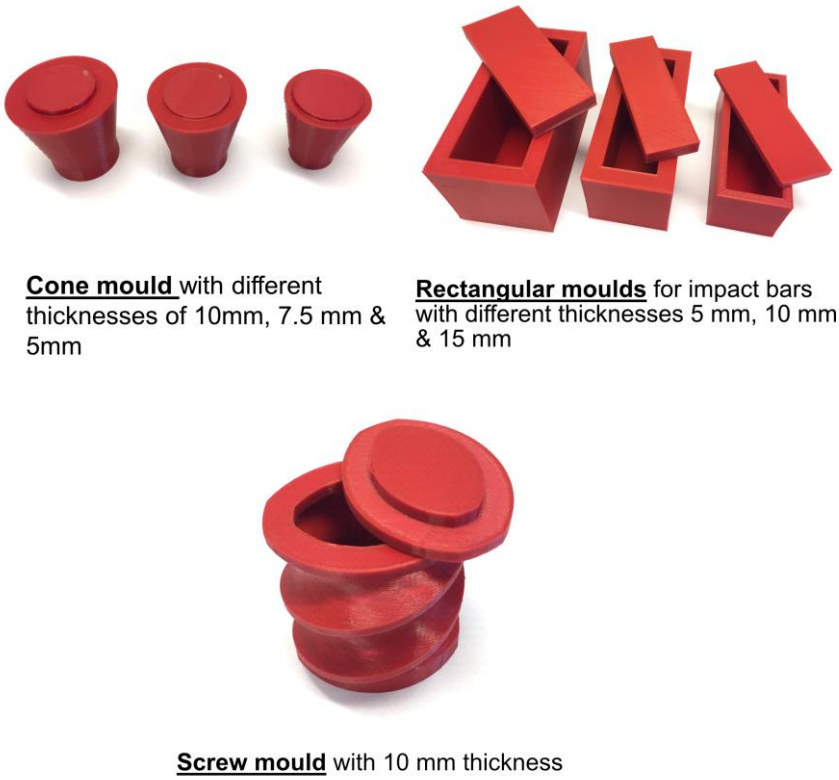

Figure 2. The 3D printed moulds made from thermoplastic polyurethane filaments using ZYYX+ FDM printer.

As seen in Figure 3, CIP trials were made using these moulds filled with metal powder. The powder grade used are CrA-2Ni-0.3C and Vanadis 4E. The CIP was done at 600 MPa on CrA-2Ni-0.3C using the QFP35L-600 machine at Quintus Technologies AB, Sweden and at 350 MPa on Vanadis 4E using Avure Technologies at RISE AB, Sweden. Before CIP, the powder was filled in these moulds and placed it in a bag for evacuation. Later, this bag was placed in chamber and underwent CIP process using water as pressure medium. It is evident that intricate shapes could be CIP-processed using the flexible FDM printing.

Screw moulds with 5 mm thickness

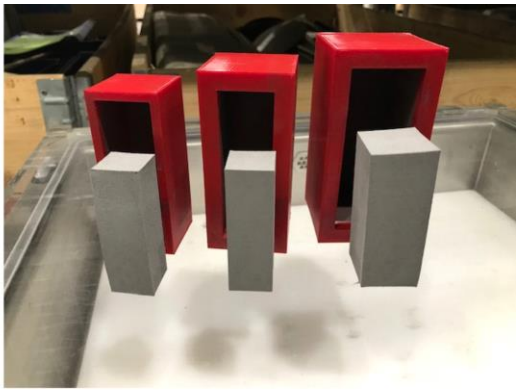

Rectangular moulds with 5 mm thickness

Punch moulds with 5 mm thickness

Figure 3. CIP process applied on complex flexible shapes

3.1.2 CIP, Sinter and Capsule-free HIP Approach for Cr-alloyed steel

1. Water-atomized Cr-prealloyed powder (known as CrA) admixed with 2 wt.% nickel and 0.3 wt.% UF-4 natural graphite from Höganäs AB was used. The addition of nickel was done by means of diffusion alloying method by Höganäs

AB. The chemical composition of the powder grade including the added carbon is provided in Table 1.

Table 1 Composition of Cr-alloyed steel powder with admixed nickel and graphite in wt.%
C* = carbon in the form of graphite

Powder	Fe	Cr	Ni	C*	O	N	S
CrA-2Ni-0.3C	Bal.	1.8	2	0.3	0.15	0.007	0.002

An overview SEM image of the aforementioned powder grade termed CrA-2Ni-0.3C powder mix can be seen in Figure 4 below.

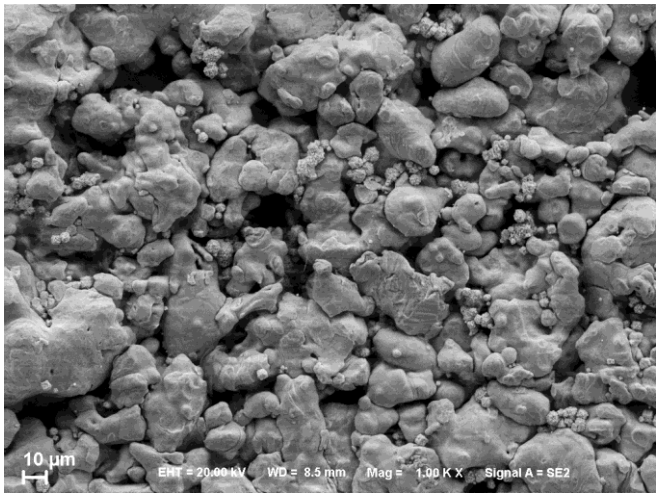

Figure 4. Overview of Cr-alloyed steel powder diffusion-bonded with 2wt%Ni and admixed with 0.3wt%C.

The CIP specimens of cylindrical shape were prepared by placing the powder samples in CIP moulds in vacuum sealed bags using water as pressure media. All the CIP specimens were produced using flexible rubber moulds of 27 mm height and 19 mm diameter in QFP35L-600 at Quintus Technologies AB, Sweden. The CIP pressures applied were 300 MPa, 450 MPa and 600 MPa, respectively, for 120 seconds of holding time per cycle. The sintering was performed in NETZSCH DIL 402C dilatometer at two different conditions: in $90N_2/10H_2$ atmosphere at 1120 °C and 1250 °C and in vacuum at 10^{-2} mbar at 1250 °C and 1350 °C, respectively. For both the conditions, heating rate of 10 °C/min and cooling rate of 30 °C/min were used with 60 min of holding time for the isothermal stage. Capsule-free HIP of the sintered specimens were carried out in QIH121 furnace at Quintus Technologies AB, Sweden using argon gas by applying pressure of 100 MPa at 1150 °C for 120 minutes. All the samples were after HIP normalized by heat treating to 960 °C in N_2 atmosphere for 60 min of holding time during the isothermal stage. This was done in order to compare role of processing with respect to defect/pore content and eliminate the role of microstructure. For

application purposes, the normalizing treatment is not a common approach, where rather there is an adjusted heat treatment for the application intended. A schematic diagram of the basic processing route is shown in Figure 5.

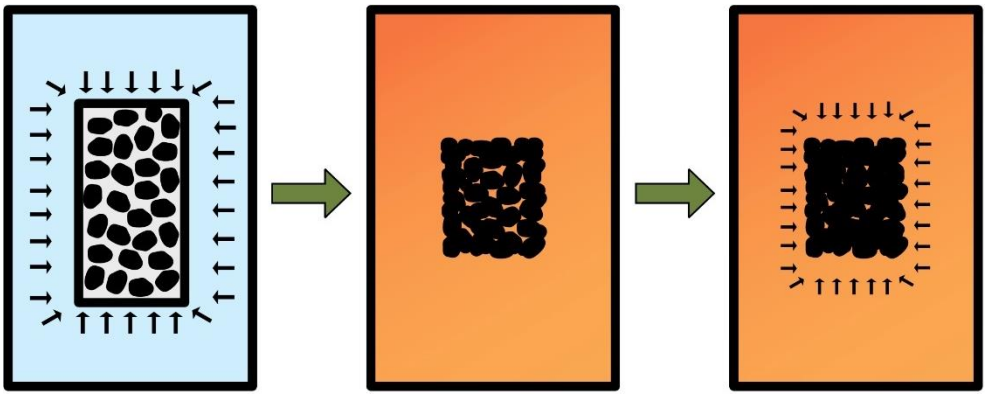

Figure 5. Schematics of procedure to obtain high density via cold isostatic pressing (CIP), sintering and capsule-free hot isostatic pressing (capsule-free HIP).

3.1.3 Compaction and Sintering Approach for Cr-alloyed steel – role of Ni

In order to evaluate the effect of Ni addition, the water atomized CrA powder without and with 2 wt.% added Ni was processed by conventional uniaxial compaction followed by sintering. Also, in this 0.3 wt.% UF-4 natural graphite was admixed to the powder variants but owing to use of uniaxial compaction instead of CIP, 0.6 wt.%

Intralube® E lubricant was also applied. Compaction was done by Höganäs AB, Sweden. The nominal chemical compositions of the variants studied are given in Table 2.

Table 2: Chemical Compositions in wt.% of the powder variants without and with added Ni, C* = Carbon in the form of graphite

Materials	Cr	Ni	C*	O	Fe
CrA-0.3C	1.8	-	0.3	0.15	Bal.
CrA-2Ni-0.3C	1.8	2	0.3	0.15	Bal.

The compacts of the two powder grades were prepared by uniaxial pressing into cylindrical shape with dimensions of 10 mm height and 10 mm diameter, and in the form of Charpy impact bars with dimensions of 10 x 10 x 50 mm^3 according to ISO 5754. Compaction was done using pressure of 550 MPa to green density of 7.1 g/cm^3. After compaction, lubricant was removed from the samples by delubrication at 450 °C for 30 minutes in dry nitrogen atmosphere. The sintering runs were then performed

at 1120 °C and 1250 °C in a NETZSCH DIL 402C dilatometer in $90N_2/10H_2$ atmosphere for 60 minutes of holding time at isothermal stage. For both materials, heating rate of 10 °C/min and cooling rate of 30 °C/min were employed.

3.1.4 Granulation, sintering and capsule-free HIP of gas-atomised tool steel powder

Gas-atomized tool steel powder of grade Vanadis 4E with size distribution of < 20 μm from Uddeholm AB was explored as prototype material for processing following the route of CIP, sintering and final capsule-free HIP. Chemical composition is given below in Table 3. To accomplish the aforementioned processing route, granulation of the spherically shaped powder to allow for CIP is a necessary must. Compressibility of the spherical powder, when having high hardness as in the case in question, is strongly restricted as there is particle interlocking during compaction. Trails were done trying to compact this powder uniaxially, but this was not successful in obtaining any appropriate green strength. Hence, granules of the powder were prepared using freeze granulation technique as described in section 2.3. Mixes with varying content of Halt B-26 binder from 10 vol.% to 30 vol.% were prepared and the compaction was compaction with binder content of 25 vol% that was shown to be enough functional.

Table 3. Nominal Composition of gas-atomized tool steel powder (Vanadis 4E)

Powder	C	Si	Mn	Cr	Mo	V	Fe
Vanadis 4E	1.4	0.4	0.4	4.7	3.5	3.7	Bal.

The granules were pre-pressed uniaxially at 20 MPa to shape them into cylindrical form. These samples were then placed in a vacuum seal bag, before being CIP-processed at 350 MPa for 120 seconds per cycle in a laboratory cold isostatic press, Avure Technologies at RISE AB, Sweden. All the CIP specimens produced were in dimensions of 10 mm in height and 10 mm diameter. Debinding of the CIP samples were done in a quartz tube furnace at 600 °C for 60 minutes in argon gas. The sintering trials were then performed in NETZSCH DIL 402C dilatometer at three different temperatures of 1150 °C, 1200 °C and 1250 °C in 100% N_2 atmosphere. The reason for selecting nitrogen as sintering atmosphere is that the nitrogen absorption into tool steel is expected to widen the sintering window and make liquid phase sintering more controllable. Heating rate of 10 °C/min and cooling rate of 30 °C/min were used with 60 min of holding time during isothermal stage for all the CIP samples. Later, Capsule-free HIP of the sintered specimens were carried out in QIH-48 furnace at Uddeholms AB, Sweden, using argon gas by applying pressure of 150 MPa at 1140 °C for 90

minutes. Tempering after capsule-free HIP samples was performed at 525 °C with 120 minutes of holding time.

3.2 Analytical Techniques

This section summarises the analysis employed in this thesis study. If not otherwise stated, the analyses were employed at the Department of Industrial and Materials Science, Chalmers University of Technology, by the author.

3.2.1 Dilatometry (DIL)

The dimensional change of a specimen is accurately measured by dilatometry as function of temperature and time. For heating cycle this means the total effect of linear sintering shrinkage and thermal expansion as well as contraction/expansion owing to phase changes [60]. The instrument used for the dilatometer experiments is a DIL 402C from NETZSCH (NETZSCH-Gerätebau GmbH, Germany) equipped with W-Re thermocouple for inert or reducing atmosphere and S-thermocouple for vacuum. The horizontal push rod dilatometer is connected to displacement transducer, which converts the linear displacement into measurement signals with a high resolution of up to 0.125 nm or 1.25 nm, depending on the range of measurement. For analysis, the specimen is placed in alumina holder and the horizontal push rod is positioned directly against the holder with a minimum force of 25cN. The dilatometer chamber is connected to the rotary and turbo pumps in sequence to perform sintering at vacuum down 10^{-4} mbar. The instrument is evacuated and flushed with argon gas up to three times before each measurement to reduce air residues. For the experiments employed, the specimen dimensions used were approximately 15 mm in height and 12 mm in diameter. To evaluate the progress of sintering, sintering runs were performed to final temperatures of 800 °C, 960 °C, 1120 °C, 1250 °C and 1350 °C in the various conditions ranging from $90N_2/10H_2$ to vacuum.

3.2.2 Thermogravimetry (TG)

Thermogravimetry (TG) is a thermoanalytical technique used for monitoring change in mass of a specimen as function of temperature [61]. During TG analysis, the changes in the specimen mass is recorded as the specimen is heated/cooled to specific temperatures with controlled heat and cooling rates. The instrument used for thermogravimetric experiments is a simultaneous TGA/DTA/DSC analyser STA 449 F1 Jupiter from Netzsch (NETZSCH-Gerätebau GmbH, Germany). Before starting the experiment, specimen of mass of about 2000 mg is collected into an alumina crucible, which is placed inside the instrument. Like mentioned for DIL 402C, the TG instrument can be evacuated using turbo pump backed with rotary pump and the chamber is usually flushed with argon gas up to three times before each measurement

to reduce air residues before setting the atmospheric conditions for the experiment. The TGA runs were in this way performed in $90N_2/10H_2$ atmosphere in SiC tube furnace with a W-Re thermocouple to monitor the temperature. These experiments were carried out at 1120 °C and at 1250 °C.

3.2.3 Density Measurements

Archimedes water displacement technique according to ASTM B328 was used for measuring density of the samples. The measurements were done on green (after CIP), sintered and HIP samples. Weight of the sample was measured in air, then followed by measuring weight in water using a setup balance of 0.0001 g accuracy. The density of the sample is calculated according to:

$$\text{Density, } \rho = \frac{W_a \, X \, \rho_w}{W_a - W_w} \text{ (in g/cm}^3\text{)} \qquad (1)$$

Where W_a and W_w are the weights of the samples in air and water measured in grams, ρ_w is the density of the water (1 g/cm^3). To seal the open pores, samples were impregnated with paraffin wax before the measurements.

3.2.4 Helium Gas Pycnometry

Helium gas pycnometer is operated on the principle of Boyle's law through which true density of the sample is measured. Helium is most widely used because of its smaller molecular size, which means that the helium molecule can penetrate through almost every pore down to atomic scale, considering its ideal gas behaviour as well. The AccuPycII 1340 He-pycnometer instrument was used at Höganäs AB. The true density measured using this technique provides the closed porosity of the samples.

3.2.5 Light Optical Microscopy

Light optical microscopy (LOM) is a technique in which visible light is used as a source, illuminated on the surface of a sample for topography, phase composition or feature contrast. The instrument used to capture the LOM images is the ZEISS Axioscope 7 equipped with digital camera for further analysis. Samples for investigation were prepared by mounting with a conductive resin, PolyFast from Struers, using hot mounting machine from Citropress-20, Struers. Grinding and polishing of these samples were done on Struers TegraPol-31 machine. The grinding was done using SiC paper of 320-grit, 500-grit, 1000-grit, 4000-grit in sequence and polishing was done using suspended diamond solutions of 9 μm, 3 μm and 1 μm in steps. Mirror-like surfaces are in this way achieved after final polishing step. In this study, LOM is carried out on sample after sintering and HIP. Etching of these samples

was done using 2% Nital to reveal the microstructure. However, porosity analysis was performed on polished samples before etching.

3.2.6 Scanning Electron Microscopy

Scanning electron microscopy (SEM) is used for high spatial resolution imaging. The high magnification provides information about surface topography and microstructural features. The fundamental principle of SEM involves directing the electron beam from source onto the surface of the sample. Thus, different type of radiations is generated such as Auger electrons (AE), secondary electrons (SE), back-scattered electrons (BSE) and X-rays. In this study secondary electron (SE) imaging was used for microstructural features and surface topography of the powder and bulk samples, chemical analysis, and mapping. The work presented in this thesis has been performed using a Gemini SEM 450 Zeiss instrument equipped with X-ray energy dispersive spectroscopy (EDS) employed for chemical analysis.

3.2.7 Chemical Analysis

Chemical analysis was performed at Höganäs AB for bulk oxygen and carbon concentration of powder, sintered samples, and HIP samples of the Cr-aloyed materials using LECO TC-600 and LECO CS-844 instruments. For oxygen analysis, the sample was heated in a graphite crucible in helium gas, during which interaction between the oxygen and carbon from the crucible takes place resulting in release of CO and CO_2. This escaped gas mixture is detected by the IR detectors, which indirectly then measures the oxygen content. The carbon analysis was performed in an induction furnace with oxygen flow where sample is combusted. The carbon from the sample reacts then with the oxygen forming CO and CO_2 gas, which is again detected by the IR detectors to determine the carbon content.

Chemical analysis was performed for bulk carbon and sulphur content of sintered and HIP samples of PM tool steel using LECO CS-600 instrument through combustion process at Uddeholms AB. The oxygen and nitrogen levels were determined using LECO ONH836 through melt extraction process.

3.2.8 Hardness Testing

Hardness of a material is defined as the measure of materials resistance to plastic deformation on indentation. In this thesis study, Vickers hardness technique was used. This technique uses a diamond shaped indenter with an angle of 136° between the faces and the tests were employed on sintered and HIP samples. A pre-defined load (L) is applied on the sample and the average diagonals lengths of the indentation on the sample are measured. According to the ASTM E384-17 standard, hardness value is calculated as follows:

$$HV = 1.8544 \frac{L}{d^2} \qquad (3)$$

where HV is the Vickers hardness in HV, L is the load applied in kgf and d is the average diagonal length of the indentations, in mm. The equipment used was Struers Durascan-70 G5 instrument for both Cr-alloyed steel and tool steel samples.

3.2.9 Impact Testing

Impact testing was done on IE bars prepared according to ISO 5754 using Instron PW 30 impact testing machine to evaluate impact energy values. These analyses were performed on 5 samples for each condition at Höganäs AB.

CHAPTER 4

RESULTS

The results section comprises two main parts. The first part is the comprehensive summary of the results from the appended papers addressing the processing route from water-atomized Cr-alloyed steel powder to full density. The second part summarizes the preliminary findings for gas-atomized tool steel following the same route.

4.1. Summary of appended papers

This section summarises the results from the appended papers. Paper I is focused on the densification behaviour of PM steel containing 1.8wt.% Cr through the route CIP→Sinter→Capsule-free HIP. Analysis of the sintering behaviour for different sintering atmospheres and temperatures was therefore investigated. As alloying with Ni is crucial for the microstructure control for the aforementioned Cr-alloyed PM-steel, the role of Ni on sintering behaviour was addressed in Paper II. The scope then is to study how admixing of 2wt.% Ni to the powder before compaction affects the shrinkage behaviour and how the densification alone impacts on mechanical properties such impact energy and hardness. Paper III finally addresses the novel alternative processing route for Cr-alloyed PM steel when sintering after CIP is performed in HIP furnace in combination with proceeding capsule-free HIP in sequence and how this aids densification, microstructure control and tentative properties.

4.1.1. Papers I and III – Densification of Cr-alloyed PM steel towards full density

The scope of the paper I was to investigate the densification behaviour of Cr-alloyed PM steel depending on processing route. Sintering in either $90N_2/10H_2$ or vacuum (10^{-2} mbar) of samples that were cold isostatically pressed at 300 MPa, 450 MPa or 600 MPa was performed at different temperatures. The plots in Figure 6 show how the relative density varies as a function of applied CIP pressure and sintering temperature. Green density after CIP increased to 7.2 g/cm^3 with the increase in isostatic pressure to 600 MPa owing to the improved mechanical interlocking between the irregularly-shaped water-atomized metal particles [40]. In Fig. 6(a) and 6(b), results for the sintering at higher temperature of 1250 °C in $90N_2/10H_2$ and vacuum (10^{-2} mbar) exhibited promising results in terms of reaching closed porosity. The important interesting finding is that surface densification then has been achieved for CIP samples compacted at 600 MPa for both sintering routes at 1250 °C [19], [41]. This enabled capsule-free HIP in argon gas after sintering to reach full density. When

sintering at 1350 °C in vacuum, most of the surface pores have been eliminated at 93% of relative density.

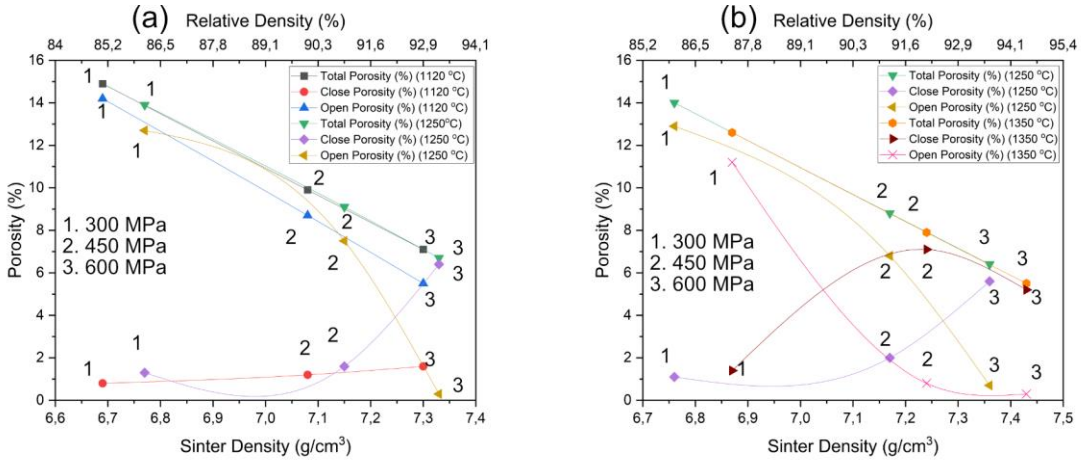

Figure 6. Plot of measured open and closed porosities as function of sintered density for sintering in (a) $90N_2/10H_2$ and (b) vacuum (10^{-2} mbar)

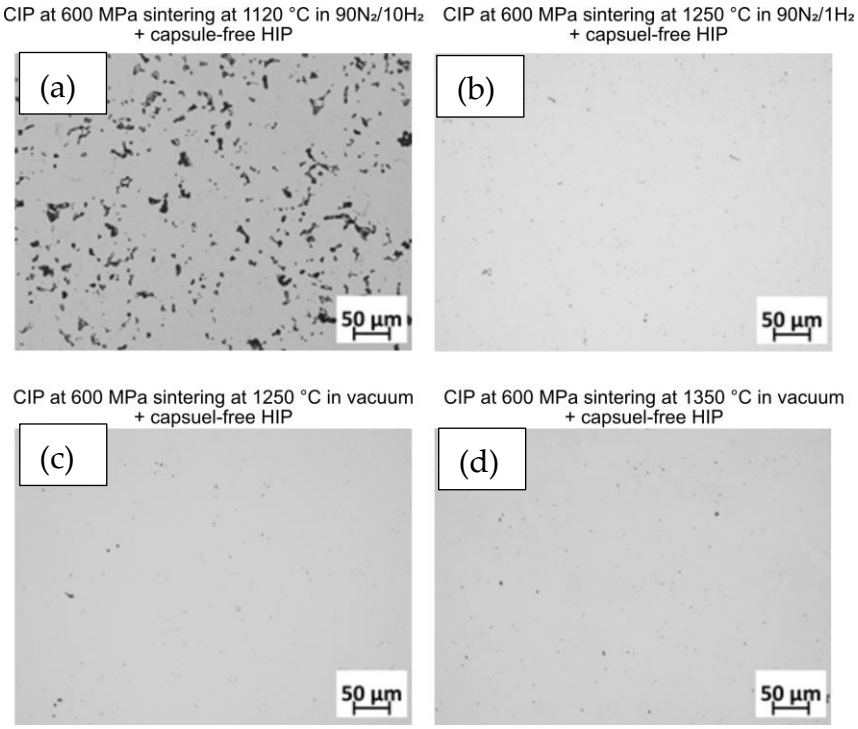

Figure 7. Pore morphology of CrA-2Ni-0.3C material after sintering and capsule-free HIP: sintering options are (a) 1120 °C in $90N_2/10H_2$, (b) 1250 °C in $90N_2/10H_2$ (c), 1250 °C in vacuum and d) 1350 °C in vacuum.

The pore morphology and its presence after capsule-free HIP of Cr-alloyed PM steel is shown in Figure 7 (Paper I). For lower temperature sintering at 1120 °C in $90N_2/10H_2$, samples contain about 5.5% pores after sintering, see Figure 7 (a). This porosity is too high to allow for appropriate densification when applying capsule-free

HIP. However, it is evident that the after capsule-free HIP, porosity fraction has drastically decreased for samples that are sintered at 1250 °C either in $90N_2/10H_2$ (Figure 7(b)) or in vacuum at 10^{-2} mbar (Figure 7(c)). This is as expected also to be observed after vacuum sintering at 1350 °C (Figure 7(d)).

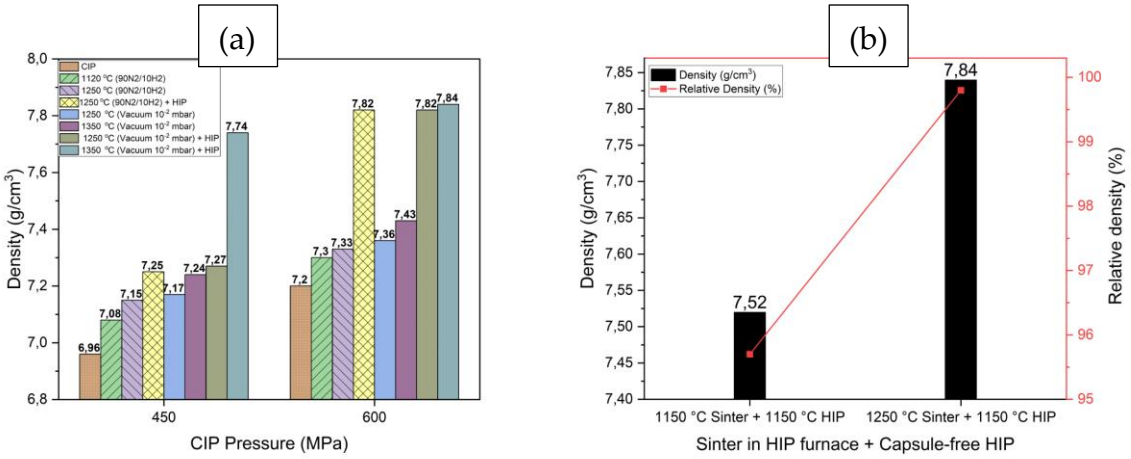

Figure 8. Density measurements of CrA-2Ni-0.3C after (a) CIP+Sinter+Capsule-free HIP (b) CIP+Sinter in HIP+Capsule-free HIP

Figure 8 illustrates the density values of the samples after sintering and capsule-free HIP process. Density values after capsule-free HIP for sample isostatically pressed at 300 MPa are not considered due to the presence of pores as seen in Figure 8(a). The results in Fig 8 (a) show that densification varies with increase in CIP pressure after sintering as well as after capsule-free HIP. Density values increased with increase in sintering temperature from 1120 °C to 1250 °C either when sintering in $90N_2/10H_2$ or in vacuum at 10^{-2} mbar at 1250 °C and at 1350 °C. It is concluded from findings in Paper I that most of surface densification is achieved at the density levels then obtained, which allowed to continue with capsule-free HIP. Similar density of 7.82 g/cm^3 is achieved for samples after capsule-free HIP when sintered at 1250 °C in $90N_2/10H_2$ and in vacuum (10^{-2} mbar). Density of 7.84 g/cm^3 is achieved after sintering at 1350 °C in vacuum (10^{-2} mbar), followed by capsule-free HP. Figure 8(b) illustrates the results from Paper III, which explores sintering in HIP furnace at 0.5 mbar vacuum followed by capsule-free HIP at 1150 °C. When sintering at 1150 °C in the HIP furnace was performed in combination with capsule-free HIP, density of 7.52 g/cm^3 was obtained, while 7.84 g/cm^3 was achieved after sintering at 1250 °C in HIP furnace followed by capsule-free HIP. The latter value indicates full or near full densification using a two-stage process in a HIP furnace without any preceding sintering.

The pore morphology of samples sintered in HIP furnace after capsule-free HIP are shown in Fig. 9(a) and 9(b). It is evident from these images that sintering at the lower

temperature of 1150 °C did not eradicate the porosity completely even after capsule-free HIP process indicating that surface densification is not achieved. Nevertheless, when sintering is performed at higher temperature 1250 °C, there are no traces of pores in the microstructure which validates the density findings in Figure 9(b) for the same sample.

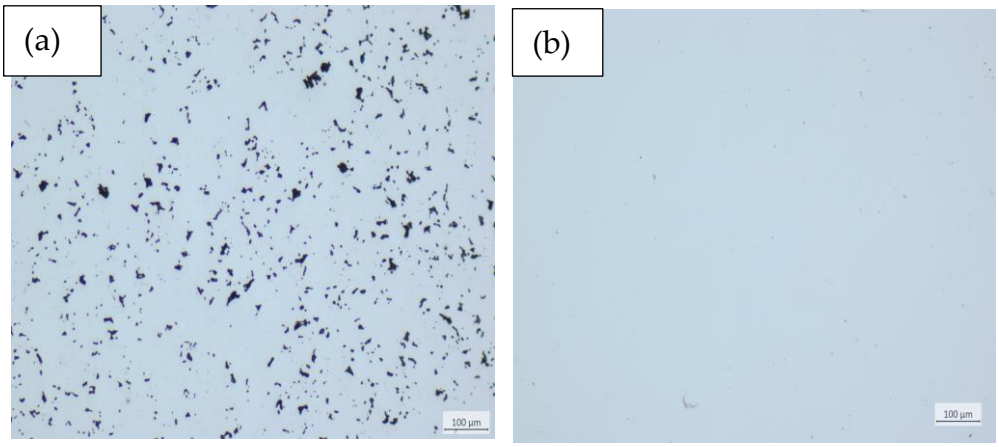

1150 °C Sinter + 1150 °C HIP **1250 °C Sinter + 1150 °C HIP**

Figure 9. light optical microscopy images of CrA-2Ni-0.3C samples after (a) 1150 °C sintering in HIP furnace + 1150 °C capsule-free HIP (a) 1250 °C sintering in HIP furnace + 1150 °C capsule-free HIP.

4.1.2 Effect of Admixed Nickel on Densification and Sintering of Cr-alloyed PM steel

The scope of this study was to investigate the role of nickel when added to Cr- alloyed steel containing 0.3% graphite, with scope on shrinkage behavior and the effect of this alone on mechanical properties. Sintering runs were done on specimens, uniaxially compacted to 7.1 g/cm^3 was done for both CrA-0.3C and CrA-2Ni-0.3C materials. The sintering was performed at 1120 °C and 1250 °C in $90N_2/10H_2$. Density values for these variants are shown in Table 4. For both materials, increase in density is as expected observed as the sintering temperature is increased. However, density was increased with the addition of admixed nickel, involving the early formation of sinter neck bridges between the metal particles during the heating stage. This has then shown to have an impact on the overall shrinkage behaviour during sintering as evidenced from Table 4. Clearly, presence of admixed Ni, most probably related to the fine Ni particle size and its homogeneous distribution is supposed to be contributors to this fact. Consequently, having admixed Ni can be expected to be beneficial for the necessary surface densification for subsequent capsule-free HIP.

Table 4 Density measurements of CrA prealloyed PM steels

Material	1120 °C	1250 °C
CrA-0.3C	7.16±0.04	7.22±0.01
CrA-2Ni-0.3C	7.23±0.01	7.28±0.01

The total dimensional changes are displayed in Table 5. Dimensional change percent is higher for the material with added nickel. This is shown for both the lower and higher temperatures of 1150 °C and 1250 °C tested, respectively. The highest shrinkage is shown for material with added nickel for the latter temperature, depicted to be 0.45±0.01%. Material without nickel shows the lowest percent shrinkage of 0.3±0.01% for the lower temperature sintering of 1120 °C.

Table 5. Total dimensional change for CrA-0.3C samples with and without nickel when sintered at 1120 °C and 1250 °C

Materials	Sintering temperature (°C)	Dimensional change (%) (DIL)
CrA-0.3C	1120	-0.3±0.01
CrA-0.3C	1250	-0.41±0.02
CrA-2Ni-0.3C	1120	-0.42±0.01
CrA-2Ni-0.3C	1250	-0.45±0.01

The apparent hardness and impact energy of CrA-0.3C and CrA-2Ni-0.3C samples sintered at 1120 °C and 1250 °C are presented in Table 6. The apparent hardness for the materials without nickel when sintered at 1120 °C and 1250 °C were 88 and 98 HV10, respectively. The apparent hardness measured for material with added nickel exhibited higher value of about 162 for both sintering temperatures. The higher hardness level is supposed to arise from two facts, the increased densification during sintering with added Ni and the presence of Ni-rich islands. The latter ones are not removed during sintering owing the limited diffusion of Ni into the Fe matrix compared to that of Fe into Ni. Also, Ni as such contribute to the overall higher hardness level.

Table 6. Apparent hardness and impact energy of CrA-0.3C with and without 2 wt.% added nickel after sintering at 1120 °C and 1250 °C

Materials	Sintering temperature (°C)	Impact energy (J)	Apparent hardness (HV10)
CrA-0.3C	1120	~45±2	88±3
CrA-0.3C	1250	~63±5	98±4
CrA-2Ni-0.3C	1120	~50±4	162±18
CrA-2Ni-0.3C	1250	~57±3	162±13

Increase in impact energy is observed as the sintering temperature is raised. The resulting impact energy for the different samples is suggested to be a combined result of porosity level and overall bulk hardness level owing to the presence of Ni-rich islands. Temperature is shown to play a major role in increasing the impact energy, while as the hardness increases with addition of nickel to CrA-0.3C, impact energy is expected to be lowered.

The EDS maps of Ni distribution for CrA-2Ni-0.3C after sintering at 1120 °C and 1250 °C are shown in Figure 10. It is clearly observed that there is heterogeneous microstructure with prevalence of Ni-rich islands for both the temperatures.

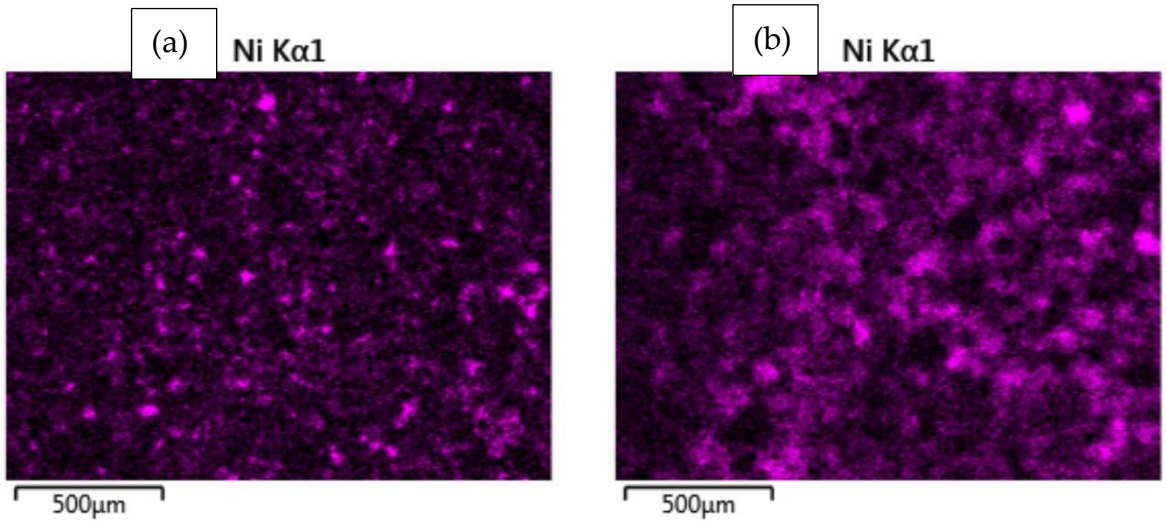

Figure 10. EDS Mapping for nickel in CrA-2Ni-0.3C after sintering at (a) 1120 °C and (b) 1250 °C

4.2. Full density processing of gas-atomized tool steel powder involving capsule-free hot isostatic pressing

The alloy known as Vanadis 4E is a cold work tool steel widely used for the application in high-performance tools exhibiting high hardness, good wear resistance and toughness. This cold work tool steel reveals uniformly distributed carbide in its homogeneous microstructure [62]–[64]. As the temperature is increased, sintering of Vanadis 4E tool steel powder is gradually activated. The material is expected to accommodate high volumetric shrinkage depending on particle size when starting from green density corresponding to ranges achievable in metal injection moulding (MIM). This improves the densification of the PM tool steel which results in higher hardness [65], [66]. Observation of post-sintering heat treatment microstructures reveal controlled formation of carbide precipitates, enabling improved hardness and strength [67]. In this thesis study, in order to increase the final density of Vanadis 4E tool steel following the route of CIP, sintering and capsule-free HIP, the effect of

sintering temperature has hence been studied in particular and full range of the processing chain has been explored.

4.2.1 Densification of Vanadis 4E PM Tool Steels Towards Full Density

Pycnometer measurements at Uddeholm AB and Archimedes density measurements at Chalmers were performed to measure closed and open porosity of sintered samples. However, pycnometer measurements are not fully accurate due to the inadequate dimensions of the tested samples, which are quite small for the pycnometer equipment available at Uddeholm AB. Hence, open, and closed porosities of Vanadis 4E after sintering and pycnometer are not shown at this stage in this thesis report.

Chemical analysis of the sintered and capsule-free HIP samples is though shown below in Tables 7 and 8. From Table 7, it can be seen that sintering temperature has not influenced the carbon content of the samples A, B and C, whereas oxygen and nitrogen has decreased with increase in sintering temperature. In fact, in all cases there is significant reduction in oxygen content suggesting that reduction of surface oxide on the original powder is highly effective. From Table 8, it is to be noted that carbon and nitrogen values after capsule-free HIP are almost like those observed for the corresponding sintered samples. On the other hand, oxygen values have reduced drastically after capsule-free HIP process for samples A and B, while the oxygen content was increased for sample C. After Capsule-free HIP, sample A has very low oxygen when compared to sample B and sample C. Still, in all cases there is low residual oxygen content.

Table 7. Chemical analysis of PM tool steel samples after sintering at 1150 °C, 1200 °C and 1250 °C

Sample	C	O	N
A	1.42	0.007	0.764
B	1.44	0.005	0.695
C	1.44	0.001	0.688

Table 8. Chemical analysis of PM tool steel samples after sintering at 1150 °C, 1200 °C and 1250 °C followed by capsule-free HIP at 1140 °C

Sample	C	O	N
A	1.46	0.001	0.74
B	1.47	0.001	0.67
C	1.44	0.004	0.65

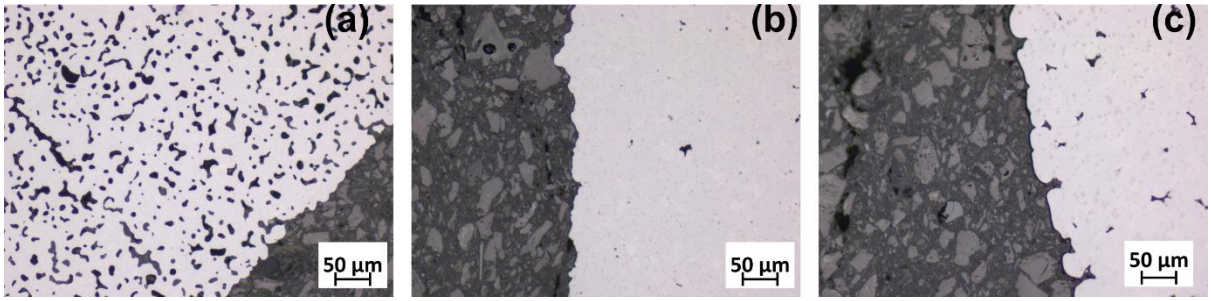

Figure 13. Pore morphology of Vanadis 4E material after sintering at (a) 1150 °C, (b) 1200 °C and (c) 1250 °C

The pore characteristics of Vanadis 4E tool steels is shown in Figure 13 as obtained after sintering at 1150 °C (Sample A), 1200 °C (Sample B), and 1250 °C (Sample C). As observed from Figure 13(a), high amount of interconnected pores are present after sintering at the lowest temperature in comparison to the results after sintering at the two higher temperatures, see Figure13(b)-(c). Still, it appears that porosity after sintering 1200 °C is lower than that after sintering at 1250 °C. At the lower of these two sintering temperatures, it can be seen from the image that complete closure of surface pores is achieved. The images validate the sintered density measurements of all the three samples as shown below in Table 9. Sample A has after sintering a density of 7.55±0.06 g/cm^3, while Sample B shows a sintered density of 7.81±0.01 g/cm^3 and sample C has then a sintered density of 7.75 g/cm^3, which is between the values of A and B samples. This illustrates that density has improved with rise in sintering temperature, except for sample C, which is suggested to be a result of over-sintering.

Table 9. Density measurements of samples A, B and C after sintering at at 1150 °C, 1200 °C and 1250 °C and after sintering, followed by capsule-free HIP and tempering

	Archimedes Density	
Sample	After Sintering (g/cm3)	After Capsule-free HIP + Tempering (g/cm3)
A	7.55±0.06	7.80±0.01
B	7.81±0.01	7.81±0.01
C	7.75±0.00	7.75±0.04

The pore characteristics of samples A, B and C after sintering and capsule-free HIP followed by tempering are shown in Figure 14. It is clear that samples A and B have no pores present, whereas sample C has surface pores. On a closer look at sample B, it appears to exhibit smoother surface when compared to other two samples (A and C). Density of the sample A after capsule-free HIP and tempering has increased to 7.80±0.01 g/cm^3, almost similar to the density of sample B which is 7.81±0.01 g/cm^3. Sample C exhibits almost same density values as in sintered stage, even after capsule-

free HIP and tempering. The values depict that after capsule-free HIP and tempering, only the density of sample A has hence increased, showing that the sintering at 1200 °C or above basically brings the material to full or near full densification.

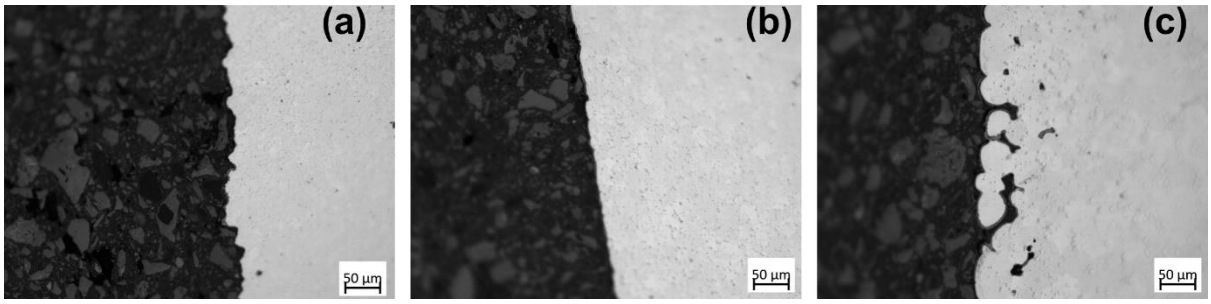

Figure 14 Pore morphology of Vanadis 4E material after sintering at (a) 1150 °C, (b) 1200 °C and (c) 1250 °C and followed by capsule-free HIP

The apparent hardness values after sintering and after capsule-free HIP, followed by tempering of sample A, B and C are shown below in Table 10. The hardness of value of sample A is 187.4±13.1 HV10 lower than hardness values of sample B, and sample C exhibiting 444±13.6 HV10 and 450±19.9 HV10 respectively. This explains clearly that porosity has an impact on the hardness of the samples after sintering at different temperatures.

Table 10. Apparent hardness measurements of samples A, B and C after sintering at 1150 °C, 1200 °C and 1250 °C and after sintering, followed by capsule-free HIP and tempering

	Hardness Measurement (HV10)	
Sample	After Sintering (g/cm3)	After Capsule-free HIP + Tempering (g/cm3)
A	188±14	519±14
B	444±14	457±11
C	450±20	458±11

Table 10 also shows the apparent hardness values after sintering, capsule-free HIP and followed by tempering. The hardness value of sample A is 520±14 HV10, which is higher than for sample B and sample C having values of 457±11 and 458±11 HV10. Although most of the pores have been eliminated for all the three samples A, B and C, the sintering, capsule-free HIP and tempering has influenced the density and hardness values.

The EDS mapping analyses of samples A, B and C after sintering are shown in Figure 15. Molybdenum and vanadium precipitates are formed at surfaces in all

temperatures after sintering, which are also formed at different depths from surface (images not shown in this thesis work).

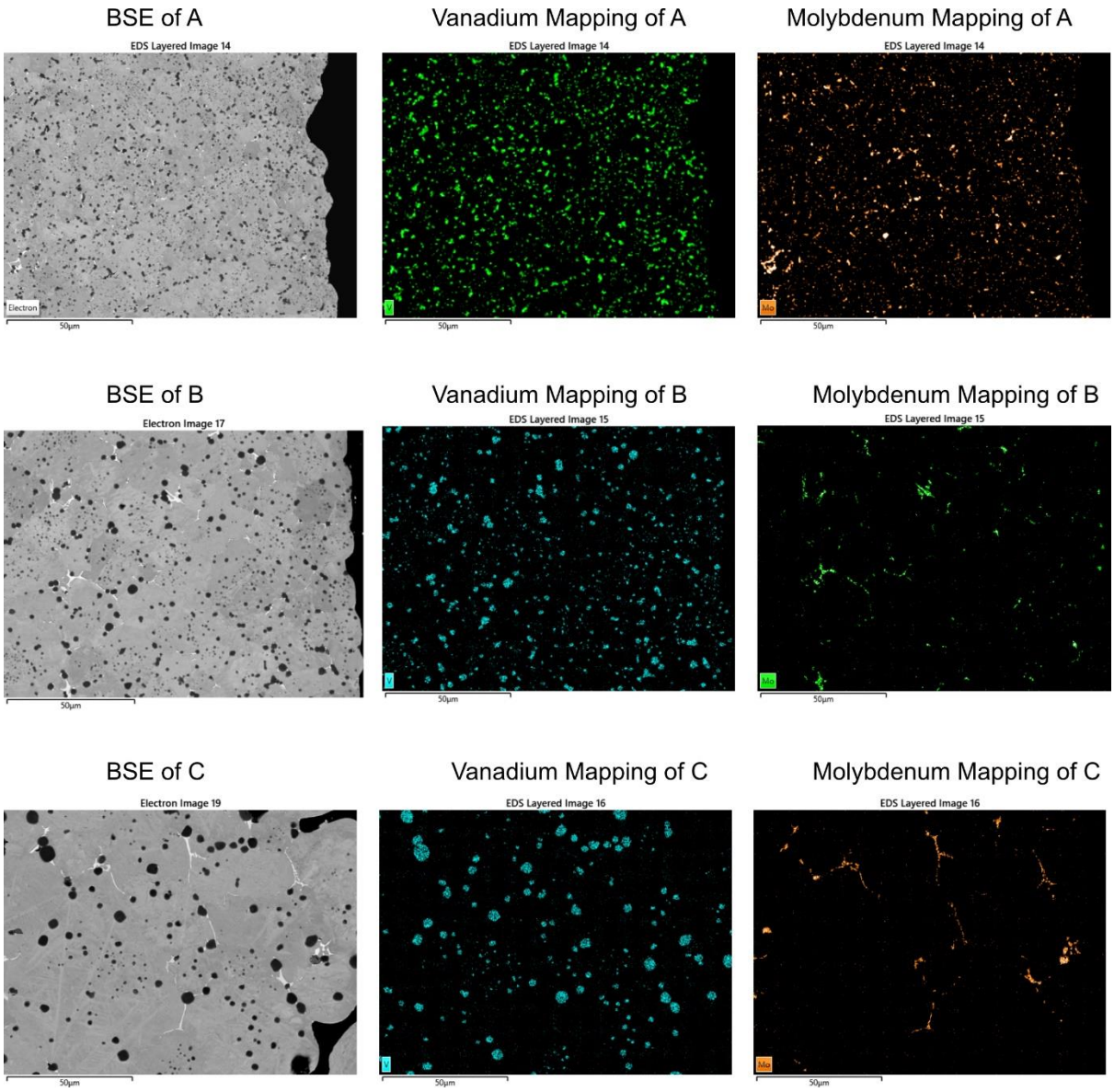

Figure 15. SEM images and EDS mapping of Vanadis 4E material after sintering at (a) 1150 °C, sample A, (b) 1200 °C, sample B and (c) 1250 °C, sample C and followed by capsule-free HIP

These precipitates formed are vanadium-rich nitrides/carbonitrides and molybdenum-rich carbides, as also observed in [72]. With increase in sintering temperature, precipitates have increased in size, especially vanadium nitrides/carbonitrides (dark spots). The precipitates formed are in line what would be expected for the alloy in question. When sintering in nitrogen atmosphere, nitrogen is dissolved into the material and VC transforms to V(C,N) and finally to VN with increasing nitrogen uptake. At the same time carbon is released and M_6C becomes the dominant carbide phase. This carbide is also Mo-rich. There tends to be higher

hardness in as-tempered condition when sintering at 1150 °C (Sample A) prior to HIP compared to those sintered at the low higher temperatures. The reason is yet unclear and will be an issue for future studies.

CHAPTER 5

CONCLUSIONS

The overall aim of this licentiate thesis has been to explore new processing route to fully densify water-atomized and gas-atomized steel powder without compromising potential near-net shape capabilities. To achieve this the overall scope has been to further explore the novel processing route combining number of processing steps, namely:

CIP →Sintering→Capsule-free HIP and CIP →Sinter in HIP→Capsule-free HIP

In particular, the use of Cr-alloyed steel with added Ni in case of water-atomized powder has been explored, while the novel processing route approach has also been proven to be viable for gas-atomised tool steel powder, but then involving granulation stage and then taking advantage of the high sintering activity of the use of fine spherical tool steel powder. Having CIP and sintering approaches established and proven to be successful for the Cr-alloyed steel with added Ni and having the benefit of Ni illustrated the scope of integrating the sintering into the HIP process and thereby eliminating a separate sintering stage has been addressed and shown to be viable to reach full density PM steel. The overall control of oxygen content has also been demonstrated with final oxygen levels indicating almost total removal of surface oxides from the original metal powder surfaces for the water-atomized Cr-alloyed steel powder. In summary, important results can hence be stated as follows.

- It is clear from the density measurements of Cr-alloyed steel after capsule-free HIP that relative density of 96% is obtained for priorly low temperature sintered (1150 °C) samples and that of 99.7% is achieved for priorly high temperature sintered (1250 °C) samples. This demonstrates the successful densification with the higher sintering temperature before the capsule-free HIP.
- This significant densification is also depicted clearly from microscopy studies showing almost no presence of pores in the samples sintered at 1250 °C followed by capsule-free HIP. From assessment of pore characteristics as function of the relative density of sintered samples, it is found that most of the open pores were eradicated after the high temperature sintering (1250 °C).
- The lower green density CIP samples when sintered at any temperature explored revealed the presence of open & closed porosities even after HIP.

- Density of 7.84 g/cm^3 (99.7% of relative density) is achieved after sintering at 1250°C in HIP furnace followed by capsule-free HIP at 1150°C.
- Admixing Ni (here 2 wt.%) to the Cr-prealloyed material has clear impact on the processing of the materials towards pre-HIP densification.
- Presence of Ni is shown to lead to activation of sinter neck formation during the heating stage as well as certain increase in overall densification corresponding to 0.05-0.1% difference in total shrinkage depending on sintering temperature explored.
- Impact energy improved with increase in sintering temperature for both the materials, CrA-0.3C and CrA-2Ni-0.3C. Impact energy was influenced with the presence of Ni-rich regions and pearlitic structure in the latter material for both sintering temperatures.
- From observed in EDS mapping of Ni distribution in the CrA-2Ni-0.3C it is shown that the heterogeneous microstructure arising from admixing is largely preserved for both sintering temperatures of 1150 °C and 1250 °C addressed.

CHAPTER 6

FUTURE SCOPE

CIP →Sinter →Capsule-free HIP Approach

- The isotropy of material properties of CIP samples should be evaluated
- Trials to facilitate further gas-atomized steel powder for CIP as heat resistant grade should be explored using freeze granulation technique
- Modelling of CIP mould design for the optimisation of shape and mould wall thickness need to be addressed to further optimise the densification of the green compact
- The manufacture and development of dimensional tolerance of gear shape demonstrators using CIP with 3D-printed polymer moulds

CIP →Sinter in HIP Furnace→Capsule-free HIP Approach

- The microstructural comparison between the results using the routes CIP+Sinter+Capsule-free HIP and CIP+Sinter in HIP furnace+Capsule-free HIP.
- The further optimization of the HIP parameters as a function of temperature, time, and pressure for water-atomized and gas atomized powder grades
- The assessment of active constituents during sintering in HIP furnace followed by capsule-free HIP
- The study of the economic feasibility of the novel approach involving CIP+Sinter in HIP furnace+Capsule-free HIP

ACKNOWLEDGEMENTS

I would like to thank my supervisors Prof. Lars Nyborg and Prof. Eduard Hryha for providing me with this opportunity and support to carry out research in powder metallurgy. I would like to extend my thanks to Prof. Yu Cao for providing guidance.

I would like to express my gratitude to Dr. Maheswaran Vattur Sundaram for all the fruitful discussions and guidance during the last couple of years.

I would like to acknowledge and extend my thanks to Dr. Michael Andersson, Dr. Dimitris Chasoglou from Höganäs AB, Dr. Hans Magnusson from Swerim AB, Dr. Erik Adolfsson and Mr. Ola Lyckfeldt from RISE IVF, Dr. Christos Oikonomou and Dr. Giulio Maistro from Uddeholm AB, Johannes Gårdstam from Quintus Technologies AB, Mr. Miles Cao, Mr. Roger Berglund from Kanthal AB for all the collaborations within the framework of this project.

I would like to thank Roger Saghdahl, Dr. Yiming Yao, Dr. Eric Tam for all the help in fixing things related technical issues whenever needed.

I would especially like to express my thanks to all fellow PhD students, past and present for sharing this journey with me.

I would like to thank my parents, sister, and my wife Preethi for their love, encouragement and support.

REFERENCES

[1] J. Capus, "Higher density, higher performance at POWDERMET2018," *Met. Powder Rep.*, vol. 73, no. 6, pp. 310–313, 2018.

[2] W. B. James and H. Corporation, "Powder Metallurgy Methods and Applications," vol. 7, 2015.

[3] J. P. Adams, "History of Powder Metallurgy," *Powder Metall.*, vol. 7, pp. 3–8, 2018.

[4] D. Ramakrishnan, *Automotive applications of powder metallurgy*. Woodhead Publishing Limited, 2013.

[5] G. Matula, T. Jardiel, R. Jimenez, B. Levenfeld, and a Várez, "Microstructure , mechanical and electrical properties of Ni-YSZ anode supported solid oxide fuel cells," *Powder Metall.*, vol. 32, no. 1, pp. 21–24, 2008.

[6] R. Bureš, M. Strečková, M. Fáberová, P. Kollár, and J. Füzer, "Advances in Powder Metallurgy Soft Magnetic Composite Materials," *Arch. Metall. Mater.*, vol. 62, no. 2, pp. 1149–1154, 2017.

[7] H.G. RUTZ, "High density processing of high performance ferrous materials," *Adv. Powder Metall. Part. Mater.*, vol. 5, pp. 117–133, 1994.

[8] J. Mascarenhas, "Powder metallurgy: A major partner of the sustainable development," *Mater. Sci. Forum*, vol. 455–456, no. May, pp. 857–860, 2004.

[9] MPIF, "Powder Metallurgy—Intrinsically Sustainable," *Met. Powder Ind. Fed.*, 2015.

[10] F. Shang, B. Qiao, H. Li, Y. He, X. Tang, and J. Yang, "Application of PM technology on manufacturing of automotive parts," *Proc. - 3rd Int. Conf. Meas. Technol. Mechatronics Autom. ICMTMA 2011*, vol. 1, pp. 563–565, 2011.

[11] C. Schade and J. J. Dunkley, "Atomization," *Powder Metall.*, vol. 7, pp. 58–71, 2018.

[12] F. Lemoisson and L. Froyen, "Understanding and improving powder metallurgical processes," *Fundam. Metall.*, pp. 471–502, 2005.

[13] D. Chasoglou, S. Hedström, and O. Bergman, "Study on the effect of alloying elements on the hardenability of PM steels," *Euro PM 2018 Congr. Exhib.*, pp. 1–7, 2020.

[14] M. Nabee, R. Frykholm, and P. Hedström, "Influence of alloying elements on Ni distribution in PM steels," *Powder Metall.*, vol. 57, no. 2, pp. 111–118, 2014.

[15] W. B. James, "Ferrous Powder Metallurgy Materials," *Powder Metall.*, vol. 7, pp. 295–310, 2018.

[16] S. Geroldinger, "Sinter Hardening PM Steels Prepared through Hybrid Alloying," *HTM - J. Heat Treat. Mater.*, vol. 76, no. 2, pp. 105–119, 2021.

[17] O. Lyckfeldt, M. Sjöstedt, and J. Orlenius, "Freeze Granulation," *Swerea IVF Prod. Sheet*, vol. 46, no. 0, pp. 1–2, 2013.

[18] R. Haynes, "Development of sintered low alloy steels," *Powder Metall.*, vol. 32, no. 2, pp. 140–146, 1989.

[19] M. Danninger, H., Zengin, Z-O., Drozda, "High Pressure Compaction of Ferrous PM Parts," *Met. Powder Rep.*, vol. 41, no. 11, pp. 833–838, 1986.

[20] N. D. Sopchak and W. Z. Misiolek, "Density gradients in multilayer compacted iron powder parts," *Mater. Manuf. Process.*, vol. 15, no. 1, pp. 65–79, 2000.

[21] R. M. German, "Green body homogeneity effects on sintered tolerances," *Powder Metall.*, vol. 47, no. 2, pp. 157–160, 2004.

[22] Höganäs AB, "Höganäs Handbook for Sintered Components Power of Powder ® Production of Sintered Components 2," 2013.

[23] A. Simchi, "Effects of lubrication procedure on the consolidation, sintering and microstructural features of powder compacts," *Mater. Des.*, vol. 24, no. 8, pp. 585–594, 2003.

[24] E. Hryha, E. Dudrova, and L. Nyborg, "On-line control of processing atmospheres for proper sintering of oxidation-sensitive PM steels," *J. Mater. Process. Technol.*, vol. 212, no. 4, pp. 977–987, 2012.

[25] E. Hryha, S. Karamchedu, D. Riabov, L. Nyborg, and S. Berg, "Effect of Active Components of Sintering Atmosphere on Reduction/Oxidation Processes during Sintering of Cr-Alloyed PM Steels," *J. Am. Ceram. Soc.*, vol. 98, no. 11, pp. 3561–3568, 2015.

[26] E. Hryha and L. Nyborg, "Process control system for delubrication of PM steels," *Acta Metall. Slovaca*, vol. 18, no. 2–3, pp. 60–68, 2012.

[27] E. Hryha, H. Borgström, K. Sterky, and L. Nyborg, "Influence of the steel powder type and processing parameters on the debinding of PM compacts with gelatin binder," *J. Therm. Anal. Calorim.*, vol. 118, no. 2, pp. 695–704, 2014.

[28] P.E: Price, "Cold isostatic pressing," *Prod Eng*, vol. 50, no. 12, pp. 515–520, 1971.

[29] "Characterising powders for CIP "Powder Metallurgy Review 2019 61-67

[30] U. M. Attia, "Cold-isostatic pressing of metal powders: a review of the technology and recent developments," *Critical Reviews in Solid State and Materials Sciences*, vol. 46, no. 6. Taylor and Francis Ltd., pp. 587–610, 2021.

[31] R. M. Govindarajan and N. Aravas, "DEFORMATION PROCESSING OF METAL POWDERS: PART I-COLD ISOSTATIC PRESSING," 1994.

[32] O. Bergman, D. Chasoglou, and M. Dahlström, "Properties of Cr-alloyed PM steel after different sintering and heat treatment operations," *World PM 2016 Congr. Exhib.*, pp. 9–12, 2016.

[33] Linde AG, "Sintering of steels .," *Furn. Atmos.*, no. 6, 2020.

[34] E. Hryha and L. Nyborg, "Thermogravimetry study of the effectiveness of different reducing agents during sintering of Cr-prealloyed PM steels," *J. Therm. Anal. Calorim.*, vol. 118, no. 2, pp. 825–834, 2014.

[35] J. Wendel, R. Shvab, Y. Cao, E. Hryha, and L. Nyborg, "Surface analysis of fine water-atomized iron powder and sintered material," *Surf. Interface Anal.*, vol. 50, no. 11, pp. 1065–1071, 2018.

[36] "Höganäs Handbook Chapter 6 Höganäs, Sweden."

[37] E. Hryha and L. Nyborg, "Oxide transformation in Cr-Mn-prealloyed sintered steels: Thermodynamic and kinetic aspects," *Metall. Mater. Trans. A Phys. Metall. Mater. Sci.*, vol. 45, no. 4, pp. 1736–1747, 2014.

[38] H. Danninger, G. Frauendienst, K. D. Streb, and R. Ratzi, "Dissolution of different graphite grades during sintering of PM steels," *Mater. Chem. Phys.*, vol. 67, no. 1–3, pp. 72–77, 2001.

[39] D. F. Heaney, "Vacuum sintering," in *Sintering of Advanced Materials*, Elsevier, 2010, pp. 189–221.

[40] M. G. and Y. T. F. Gosselin, "P/m steels," *PM Steels, Adv. Powder Metall. Part. Mater.*, vol. 5, no. 609, pp. 127–140, 1992.

[41] M. Vattur Sundaram, E. Hryha, D. Chasoglou, A. Rottstegge, and L. Nyborg, "Effect of Density and Processing Conditions on Oxide Transformations and Mechanical Properties in Cr–Mo-Alloyed PM steels," *Metall. Mater. Trans. A Phys. Metall. Mater. Sci.*, vol. 53, no. 2, pp. 640–652, 2021.

[42] U. Engström, "Influence of sintering temperature on properties of low alloyed high strength PM materials," *Adv. Powder Metall. Part. Mater.*, pp. 1418–1429, 2001.

[43] O. Bergman, D. Chasoglou, and M. Dahlström, "Mechanical performance of Cr-alloyed PM steel after different sintering and heat treatment operations," *Met. Powder Rep.*, vol. 73, no. 1, pp. 21–25, 2018.

[44] E. Bernardo, M. Campos, J. M. Torralba, C. Gierl, H. Danninger, and R. Frykholm, "Lean steels modified with a new Cu-based master alloy: Influence of process parameters in dimensional and sintering behavior," *Int. Powder Metall. Congr. Exhib. Euro PM 2013*, 2013.

[45] M. W. Wu, K. S. Hwang, and K. H. Chuang, "Improved distribution of nickel and carbon in sintered steels through addition of chromium and molybdenum,"

Powder Metall., vol. 51, no. 2, pp. 160–165, 2008.

[46] M. W. Wu and K. S. Hwang, "Improved homogenization of Ni in sintered steels through the use of Cr-containing prealloyed powders," *Metall. Mater. Trans. A Phys. Metall. Mater. Sci.*, vol. 37, no. 12, pp. 3577–3585, 2006.

[47] M. W. Wu, L. C. Tsao, G. J. Shu, and B. H. Lin, "The effects of alloying elements and microstructure on the impact toughness of powder metal steels," *Mater. Sci. Eng. A*, vol. 538, pp. 135–144, 2012.

[48] F. Hanejko, "Single press/single sinter solutions to high density," *Powder Metall.*, vol. 53, no. 2, pp. 100–102, 2010.

[49] G. F. Bocchini, "The influences of porosity on the characteristics of sintered materials," *SAE Tech. Pap.*, no. May, 1986.

[50] Höganäs, "Design and mechanical properties," *Höganäs Handb. sintered components*, vol. 3, p. 128, 2013.

[51] T. Marcu, A. Molinari, G. Straffelini, and S. Berg, "Microstructure and tensile properties of 3%Cr-0·5%Mo high carbon PM sintered steels," *Powder Metall.*, vol. 48, no. 2, pp. 139–143, 2005.

[52] E. Hryha and L. Nyborg, "Microstructure development in powder metallurgy steels: Effect of alloying elements and process variables," *Mater. Sci. Forum*, vol. 782, pp. 467–472, 2014.

[53] C. Lindberg, "Mechanical properties of warm compacted astaloy CrM," *Adv. Powder Metall. Part. Mater.*, vol. 3, no. 6/9, pp. 6–81, 2000.

[54] C. Barre, "Hot isostatic pressing," *Adv. Mater. Process.*, vol. 155, no. 3, pp. 47–48, 1999.

[55] J. James, "Hot isostatic pressing : an economic route to powder components," no. November, 1977.

[56] W. R. Morgan and R. L. Sands, "Isostatic compaction of metal powders," *Kov. Mater.*, vol. 14, no. 1, pp. 85–102, 1969.

[57] S. J. Mashl, J. C. Hebeisen, and C. G. Hjorth, "Producing large P/M near-net shapes using hot isostatic pressing," *Jom*, vol. 51, no. 7, pp. 29–31, 1999.

[58] M. Andersson *et al.*, "Manufacturing full density powder metallurgy gears through HIP:ing," *Met. Powder Rep.*, vol. 74, no. 4, pp. 199–203, 2019.

[59] A. Leicht *et al.*, "As-HIP microstructure of EBM fabricated shell components," *World PM 2016 Congr. Exhib.*, p. 2016, 2016.

[60] K. Maca, V. Pouchly, and A. R. Boccaccini, "Sintering densification curve - A practical approach for its construction from dilatometric shrinkage data," *Sci. Sinter.*, vol. 40, no. 2, pp. 117–122, 2008.

[61] P. J. Haines, *Thermal Methods of Analysis: Principles, Applications and Problems*. 1995.

[62] I. Gunes et al, "Evaluation of wear performance of cryogenically treated Vanadis 4 Extra tool steel," *Kov. Mater.*, vol. 54, pp. 1–10, 2016.

[63] F. K. Arslan, I. Altinsoy, A. Hatman, M. Ipek, S. Zeytin, and C. Bindal, "Characterization of cryogenic heat treated Vanadis 4 PM cold work tool steel," *Vacuum*, vol. 86, no. 4, pp. 370–373, 2011.

[64] S. H. Chang, P. T. Yeh, and K. T. Huang, "Microstructures, mechanical properties and corrosion behaviors of NbC added to Vanadis 4 tool steel via vacuum sintering and heat treatments," *Vacuum*, vol. 142, pp. 123–130, 2017.

[65] D. Godlinski and G. Veltl, "Three dimensional printing of PM-tool steels," *Euro PM 2005 Powder Metall. Congr. Exhib.*, vol. 3, pp. 49–54, 2005.

[66] S. Kremel, H. Danninger, and Y. Yu, "Effect of Sintering conditions on Particle contacts and mechanical properties of PM steels prepared from 3 % Cr prealloyed powder," *Powder Metall. Prog.*, vol. 2, no. 4, pp. 211–221, 2002.

[67] S. H. Chang, T. P. Tang, K. T. Huang, and F. C. Tai, "Effects of sintering process and heat treatments on microstructures and mechanical properties of VANADIS 4 tool steel added with TiC powders," *Powder Metall.*, vol. 54, no. 4, pp. 507–512, 2011.

[68] D. Chasoglou, E. Hryha, L. Nyborg, "Effect of process parameters on surface oxides on chromium-alloyed steel powder during sintering", Materials Chemistry and Physics 138 (2013)

[69] E. Hryha, "Application of Fractography For Investigation Of Surface Oxide Reduction/Transformation and Inter-Particle Necks Formation During Sintering of Prealloyed with Cr and Mn PM Steels", Powder Metallurgy Progress, Vol.14 (2014), No 1

[70] E. Hryha, L. Nyborg: „Oxide Transformation in Cr-Mn-Prealloyed Sintered Steels: Thermodynamic and Kinetic Aspects", *Metallurgical and Materials Transactions A*, 2014, Vol. 45, No. 4, pp. 1736-1747

[71] Z. A. Munir (1981) Surface Oxides and Sintering of Metals, Powder Metallurgy, 24:4, 177-180

[72] Henrik Borgstrom , Lars Nyborg, "Liquid Phase Sintering of Ferrous Powder Metallurgical Materials, *Proceedings of Sino-Swedish Structural Materials Symposium 2007 70-76*